Selectivity loss in Fischer-Tropsch synthesis : The effect of carbon deposition

Paul Hazemann, Dominique Decottignies, Sylvie Maury, Séverine Humbert, Frédéric Meunier, Y. Schuurman

Selectivity loss in Fischer-Tropsch synthesis: the effect of carbon deposition

Paul Hazemann,[a,b] Dominique Decottignies,[a] Sylvie Maury,[a] Séverine Humbert,[a] Frederic C. Meunier,[b] Yves Schuurman* [b]

[a] *IFP Energies nouvelles, Rond-Point de l'Echangeur de Solaize−BP3, Solaize 69360, France*
[b] *Univ Lyon, Université Claude Bernard Lyon 1, CNRS, IRCELYON, F-69626, Villeurbanne, France*

Abstract

Polymeric carbon was deposited over Siralox supported cobalt catalysts by an ethylene treatment at 230°C and 260°C. Cobalt catalysts with cobalt particle sizes of 10 and 14 nm were studied. Temperature programmed hydrogenation and Raman spectroscopy analyses of the deposited species were found to be similar to those formed during Fischer-Tropsch synthesis. The cobalt catalysts were tested in high-throughput 16 parallel reactors at 20 bars and 220°C, using a H_2/CO ratio of 2.12. Data were collected at different space times to compare activities and selectivities at iso-conversion levels. Ethylene treated catalysts showed lower activity that corresponded roughly to the loss of CO adsorption sites. Additionally, a decrease of the heavy products selectivity, an increase in the methane selectivity and a decrease of the olefin to paraffin ratio was observed after the ethylene treatments. Unlike the loss in activity, the deselectivation level was found to depend on the amount of deposited carbon. This phenomenon can be explained by a steric effect of the deposit, but an electronic effect cannot be excluded, but is challenging to prove.

Keywords: *ethylene-treatment; deactivation; Co catalysts; high-throughput experiments*

Introduction

Catalyst deactivation is of a great concern in most industrial processes, because it implies to replace or to regenerate frequently the catalyst [1]. In Fischer-Tropsch catalysis, this loss of activity is moreover accompanied by a deselectivation phenomenon [2,3]. Heavy product selectivity decreases with time on stream whereas methane selectivity increases. A lot of interest has been devoted to Fischer-Tropsch catalyst deactivation in the past decades, and

*corresponding author: yves.schuurman@ircelyon.univ-lyon1.fr

different phenomena that causes a selectivity shift have been reported [4–6]. It is of common knowledge that deactivation can result from a combination of several phenomena [4,6] : carbon deposition [7–11], active phase carburization [12–14], water induced effects (re-oxidation [15], sintering [5,16], support hydroxylation [17,18]), but also poisoning [19,20] or even surface reconstruction [5,21]. However, their respective effect on catalysts selectivity has not been specifically studied, at least not at iso-conversion levels.

Selectivity impacts of polymeric carbon deposits on cobalt catalysts at realistic FTS conditions are not well understood. The work of Sage et al. [22] yet suggested that carbon deposition, one of the main deactivation mechanisms [7,9,23], may be involved in a selectivity shift: an increase in light compounds selectivity has been observed at iso-conversion after carbon deposition on a Co/Al_2O_3 catalyst, simulated by acetylene treatment. Zhai et al. [24] also observed a selectivity shift after carbon deposition by ethylene treatments on cobalt catalysts, with an increase of light compounds selectivity. Additionally, associated DFT (Density Functional Theory) calculations [24] showed that the presence of carbon on the catalyst surface facilitates methanation and hydrogenation reactions. Chen et al. [25] measured a contradictory effect, with an increase of heavy compounds selectivity after carbon deposition on a $Co\text{-}Pt/SiO_2$ catalyst, by CO treatment. They explained this behaviour by the preferential poisoning of planar surfaces, considered as the active sites for methanation only.

The divergence of these results does not allow to clearly rule on the carbon deposition effect on cobalt catalysts selectivity, moreover, the method used to simulate carbon deposition could play an important role. Carbon deposition through CO treatment may indeed be highly coordinated site-selective [25], while carbon deposition through acetylenic treatments is rather weakly coordinated site-selective [22]. This hypothesis suggests two mechanisms of carbon formation, as proposed by Bartholomew [26], who distinguished two main forms of carbon. A first kind, referred as “coke”, is generated by CO decomposition while a second kind called “carbon” is the result of hydrocarbons polymerization [10,27–29].

Recently we have investigated the role of carburization on the selectivity of cobalt FT catalysts [30]. The present study aims at characterizing carbon species deposited by ethylene polymerisation and its effect on cobalt catalysts properties. In particular, the site specificity of the carbon deposition will be studied by DRIFTS to test the hypothesis of site selectivity, and thus to rationalize the contradictory results of Chen et al. [25] and Sage et al. [22]. Catalytic tests were carried out to assess the carbon deposition involvement in catalysts deselectivation, and the underlying mechanisms will be discussed.

2. Experimental

2.1 Catalysts synthesis

Two 15 wt.% cobalt catalysts were synthetized via incipient wetness impregnation of a commercial Siralox5 support (silica-doped alumina), using a $Co(NO_3)_2 \cdot 6H_2O$ aqueous solution as a cobalt source. Two successive impregnations were necessary to reach the desired cobalt loading. After each impregnation step, the two catalyst precursors were dried and calcined in order to free porosity for further impregnation. Two different drying and calcination protocols were used in order to tune the average cobalt particles sizes, as shown by van de Loosdrecht et al. ["Calcination of Co-Based Fischer–Tropsch Synthesis Catalysts", J. van de Loosdrecht S. Barradas, E.A. Caricato, N.G. Ngwenya, P.S. Nkwanyana, M.A.S. Rawat, B.H. Sigwebela, P.J. van Berge & J.L. Visagie, Topics in Catalysis 26, 2003 121-127] have shown the impact of the space velocity and gas composition during the calcination step on the cobalt particle size. The first catalyst (referred as Co-13) was dried 12 hours in a static oven at 85°C, and then calcined for 2 h in a fixed bed reactor using air with a GHSV (Gas Hourly Space Velocity) of 2 $NL \cdot h^{-1} \cdot g^{-1}$ at 400°C (heating ramp of 2.5°C·min^{-1}). The second catalyst (referred as Co-18) was pre-dried for 30 minutes in a static oven at 85°C, before being further dried in a fluidized bed reactor at 100°C for 2 hours, under 0.8 $NL \cdot h^{-1} \cdot g^{-1}$ of air (heating ramp of 1.5°C·min^{-1}). Finally, calcination was conducted in the same reactor at 400°C for 2 h (heating ramp of 5°C·min^{-1}), using a similar GHSV of air.

2.2 Catalysts activation and carbon deposition

Catalyst activation was carried out directly in the catalytic test unit or in analytical devices under pure hydrogen (1.3 – 2.0 $NL \cdot h^{-1} \cdot g^{-1}$), at 400°C for 16 h using a heating ramp of 2°C·min^{-1}. A 24 h stabilization step was then applied to reach a relatively stable activity and to measure performances after the initial period of rapid deactivation [31]. This step was carried out under a syngas GHSV in the range 6.7 – 11.6 $NL \cdot h^{-1} \cdot g^{-1}$ (H_2/CO = 2.12), at 220°C and 20 barg (except for in-situ characterization experiments in which reactor configuration implies to work at atmospheric pressure).

Carbon was deposited on the catalyst after this stabilization step, by exposing the samples to a flow of pure ethylene at 230°C or 250°C for 3 h, under atmospheric pressure, with a GHSV of 0.2 $NL \cdot h^{-1} \cdot g^{-1}$. Note that ethylene-treated samples with no syngas exposure before treatments were also prepared for all ex-situ characterizations, to avoid perturbation of the analysis by waxes.

2.3 Characterization

Catalyst texture was characterized by nitrogen physisorption, using an Asap® 2420 apparatus from Micromeritics®. The specific surface area was calculated according to the BET method and the pore volume was assimilated to the nitrogen volume adsorbed at maximal pressure. Cobalt oxide (Co_3O_4) average particle sizes were estimated using X-Ray Diffraction (XRD) on calcined catalysts. Diffractograms were registered on a PANalytical X'Pert Pro® equipment using a copper source ($\lambda_{K\alpha 1}$ = 1.5406 Å). The average cobalt oxide (Co_3O_4) particle size was calculated by the Scherrer method, from which the metallic cobalt particle size was deduced considering the molar volume ratios of Co to Co_3O_4 (0.796).

Magnetization measurements were employed to estimate the fraction of metallic cobalt. Metallic cobalt exhibits a high magnetic susceptibility compared to its oxide phase [15,30–33] and by neglecting the non-metallic cobalt phases magnetization, the fraction of metallic cobalt Co^0/Co^{tot} can be estimated by:

$$Co^0/Co^{tot} = \frac{M_s}{M_{s,max}} = \frac{M_s}{\sigma \cdot m}$$

where M_s is the measured saturation magnetization (emu), $M_{s,max}$ the theoretical saturation magnetization of a fully reduced sample, calculated from the magnetic susceptibility of metallic cobalt, σ (emu·g^{-1}) and the cobalt mass of the sample, m (g). A magnetic field of 2T was used for the measurements.

Carbon deposits were characterized by Raman spectroscopy and Temperature Programmed Hydrogenation (TPH). A Renishaw Raman spectrometer was used, coupled with a 7.5 mW laser at the wavelength λ = 532 nm. The spectra were acquired during 300 s with a resolution of 0.5 cm^{-1}. For spot analysis, zones of 2 µm diameter were analysed, while for mapping about hundred spectra were registered on (32x32) µm square area. The I_g/I_d ratios were calculated directly from the areas, after it was checked that this gave the same result as by peak deconvolution.

TPH analysis of treated catalysts was performed in a 4 mm ID quartz reactor. Methane production was followed based on the m/z=15 amu signal, during the sample heating under 0.6 NL·h^{-1} of H_2, from 150°C to 600°C at 5°C·min^{-1}. Several known compositions of CH_4/H_2 mixtures were used to calibrate the m/z=15 amu signal.

Cobalt surface sites were quantified by CO chemisorption, performed in the same reactor as the one used for TPH experiments. The reduced samples were first exposed for 1 h to a flow of 50 ml·min^{-1} of Ar at 25°C, then the feed was abruptly switched to 40 ml·min^{-1} Ar,

5 $ml \cdot min^{-1}$ Kr and 5 $ml \cdot min^{-1}$ CO. The response delay between Kr and CO mass spectrometer signals was integrated to quantify the amount of CO adsorbed, assuming a 1:1 ratio of CO:Co_s.

The evolution of the adsorbed CO infrared bands after ethylene exposure was also characterized on the Co-18 catalyst by in-situ Diffuse Reflectance Infrared Fourier Transform Spectroscopy (DRIFTS). The DRIFTS experiment was performed in a high temperature cell (Harrick Scientific Corporation) equipped with KBr windows and using a Praying Mantis collector assembly. A spectrophotometer from ThermoFischer Scientific was used to acquire the DRIFT spectra (Nicolet 6700), with a resolution of 4 cm^{-1} and at least 16 scans accumulation. About 80 mg of catalyst was placed in an inox crucible. Before the DRIFTS experiment, the sample was reduced under 4 $NL \cdot h^{-1}$ of 0.25 H_2/0.75 N at 400°C for 18 hours. Stabilization and syngas re-exposure were carried out under 0.9 $NL \cdot h^{-1}$ of syngas (220°C, atmospheric pressure, H_2/CO = 2.12), and ethylene treatment at 230°C with a flowrate of 0.5 $NL \cdot h^{-1}$. The contribution of gas-phase CO was subtracted using a $CO_{(g)}$ spectrum collected at the reaction temperature (220°C) over a silica powder, as described elsewhere [32]. The DRIFTS spectra are reported as log(1/R), where R is the sample reflectance. This pseudo-absorbance gives a better linear representation of the band intensity against surface coverage than that given by the Kubelka–Munk function for strongly absorbing media such as those based on metals supported on oxides [33].

2.4 Fischer-Tropsch experiments

Evaluation of fresh and carbon treated catalysts performances was carried out in fixed bed reactors using a High Throughput Experimentation (HTE) setup, developed by Avantium. The unit description and performances calculations can be found in details elsewhere [34].

Either CO or small unsaturated hydrocarbons (ethylene, acetylene) are used in the literature to deposit carbon on cobalt catalysts [7,9,25] The use of CO requires high temperatures and simultaneous formation of cobalt carbide is hard to avoid. On the other hand, catalyst pre-treatment with acetylene or ethylene at low temperatures lead to the formation of graphene or polymeric carbon, which is associated with long-term catalyst deactivation [10,24]. Weststrate et al. pretreated a reduced cobalt catalyst with ethylene at 260°C and observed the formation of polymeric carbon and a activity loss of approximately 50%, representative for a 100 days on stream FT catalyst [10].

To characterize the fresh catalyst performances, 350 mg of oxide solids were reduced using the protocol described in section 2.2 (H_2 GHSV of 1.8 $NL \cdot h^{-1} \cdot g^{-1}$). The temperature was then decreased to 180°C under hydrogen, and the pressure progressively increased to 20 barg.

Syngas (H_2/CO = 2.12) containing 5% He was injected with a flowrate of 2.51 $NL \cdot h^{-1}$, and the temperature increased to 220°C with a heating ramp of 1°C·min^{-1}. After the 24 h stabilization step, the syngas flowrate was varied successively to measure selectivities at different conversion levels.

For carbon treated catalyst performance evaluations, a similar start-up procedure was used, but after stabilization the pressure was decreased to 0 barg under inert gas and catalysts treated at 230 and 250°C with an ethylene flow of a 0.06 $NL \cdot h^{-1}$ for 3 h. Syngas was then re-introduced, pressure increased to 20 barg and temperature also decreased to 220°C. Different gas flowrates were operated to measure performances at different conversion levels.

2.5 Wax composition analysis

The liquid products generated during HT tests were analysed and quantified off-line by simulated distillation to evaluate the corresponding chain growth probability. The hydrocarbon mix was first dissolved in CS_2 before being eluted through a MXT®-1 column, and hydrocarbons were quantified by a FID. The chain growth probability α was calculated from the C_{17-42} hydrocarbons distribution using an Anderson-Schulz-Flory (ASF) [35] fit.

3. Results

3.1 Catalysts physical properties

The two prepared catalysts exhibit similar textural properties, as shown in Table 1, with slightly lower surface area and pore volume than the support (171 $m^2 \cdot g^{-1}$, 0.52 $mL \cdot g^{-1}$). This is due to the cobalt impregnation that decreases the mass fraction of the support in the final catalyst, which decreases therefore the apparent specific surface area and pore volume.

Different average Co_3O_4 particle sizes are measured for the two catalysts by XRD (Table 1). A larger particle size is found for the Co-18 catalyst than for the Co-13 one, with a value of 18±2 nm against 13±1 nm for Co-13. The reduced catalyst average cobalt particle sizes, deduced from these values (assuming that the metal particle size corresponds to 75% of the oxide particle size), are estimated at 10±0.8 nm and 14±1.6 nm for Co-13 and Co-18, respectively. The reduction of the catalysts leads to 58% of metallic cobalt for both samples as found by magnetic measurements.

Table 1: Catalyst textural properties, cobalt particle sizes and degree of reduction (DOR).

	S_{BET} (m^2/g)	V_p (ml/g)	$d_{Co3O4,XRD}$ (nm)	$d_{Co,XRD}$ (nm)	DOR
Co-13	133	0.36	13±1	10±0.8	58 ± 3
Co-18	135	0.36	18±2	14±1.6	58 ± 3

3.2 Carbon deposition *via* exposure to ethylene

3.2.1 Raman spectroscopy

Figure 1 presents the Raman spectra obtained on the two catalysts treated at 230°C and 250°C, in the carbon frequency region.

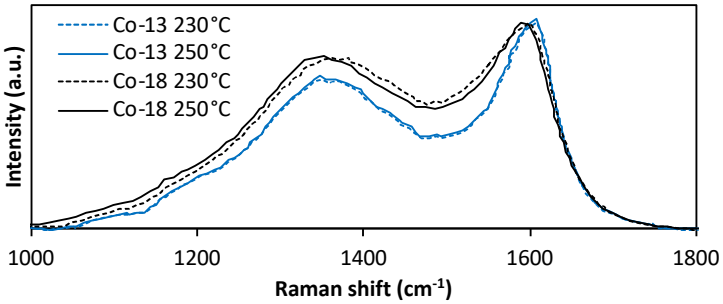

Figure 1: Raman spectra of the carbon deposited on the reduced catalysts by ethylene treatments (P_{atm}, 0.2 $NL \cdot h^{-1}$ C_2H_4).

Both D and G bands are systematically detected in each spectrum, respectively at 1350 and 1600 cm^{-1}. This indicates the presence of structured carbon but with the presence of defects. Similar spectra have been recorded on catalysts tested under real conditions for Fischer-Tropsch synthesis [8,36], the species deposited through ethylene exposure may thus be similar to the ones deposited during Fischer-Tropsch synthesis. Although Raman spectroscopy is not a quantitative analysis, the ratio of the two bands intensity I_D/I_G, can give semi-quantitative information on the concentrations of defects present in the carbon structure [8,16,36,37]. It was, however, observed that our samples were quite heterogeneous, the I_D/I_G values differed significantly depending on the location of the spotted area. Thus, for a more accurate comparison of the different samples, this ratio has been evaluated on about hundred spots for each sample. The obtained distributions of I_D/I_G for the two catalysts treated at the two temperatures are presented in Figure 2. This heterogeneity can be the results of a concentration

gradient in the fixed bed reactor, but also from a heterogeneity on the grain-scale, as the distribution depend on the cobalt particle size.

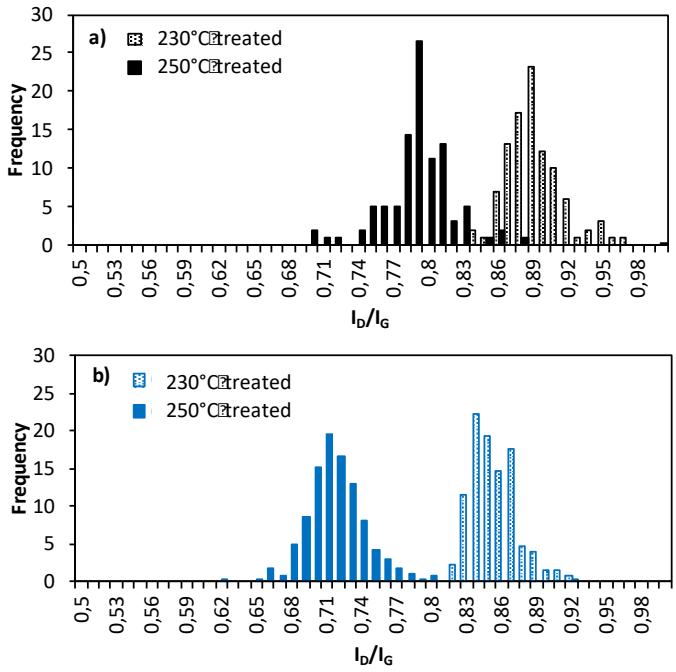

Figure 2: Ratios of D and G band intensities of the carbon deposited on the a) Co-18 and b) Co-13 catalysts by ethylene treatments.

A clear effect of the ethylene treatment temperature is observed, with lower I_D/I_G ratios for the 250°C ethylene treatment than for the 230°C one. This means that the temperature increase induces the formation of a more graphitic carbon, with less defects [8,16,22,24,36,37]. Besides, the ratios are globally lower for the Co-13 catalysts. The catalyst particle size may thus have an impact on the carbon deposit structure.

3.2.2 Temperature Programmed Hydrogenation (TPH)

To further characterize the carbon species deposited by ethylene exposure at two temperatures, TPH was performed on the different samples. The obtained profiles, presented in Figure 3, are very similar for each sample: A broad signal is observed between 100 and 550°C, indicating the presence of several types of species. Moodley et al. have proposed [7] an identification of the compounds deposited during Fischer-Tropsch synthesis based on their hydrogenation temperature, which has been widely re-used and completed by other research groups [9,23,24,38,39]. The species with hydrogenation temperatures below 250°C are considered to be weakly adsorbed hydrocarbons, the compounds hydrogenated at a temperature

around 350°C correspond to heavy hydrocarbons, and above 400°C to polymeric carbon. These last two species are the ones considered responsible for carbon-induced deactivation [7]. Deconvolution of the TPH profiles obtained herein reveals the presence of both a species that corresponds to the heavy hydrocarbons and polymeric carbon, as defined by Moodley [7]. Note that the species presented in Figure 3, are formed during ethylene pre-treatment and not during FTS, as those described by Moodley et al. [7]. The hydrogenation temperature corresponds to a similar reactivity with respect to hydrogen, but the nature of the carbon containing species during ethylene pre-treatment and FTS might be different. The "heavier hydrocarbons" probably correspond to ethylene oligomerization products. Some low hydrogenation temperature (<300°C) species are also detected, at three different hydrogenation temperatures. For both catalysts, the increase of ethylene treatment temperature induces an increase of the amount of heavy hydrocarbons and polymeric carbon deposited. No change of the amount of low hydrogenation temperature species is however measured, they might thus correspond to intermediates for the formation of long carbon chains and polymeric carbon, such as acetylenic species [10,28]. This increase of polymeric carbon deposition is in line with Raman spectroscopy results, since we observed a more graphitic-like structure on the 250°C treated samples. More precisely, the lower defaults concentration observed for these samples is the sign of a more polymerized structure, which is what has been also deduced from TPH profiles.

Some small amounts of cobalt carbide could also be formed by the ethylene treatment, but its presence is hard to prove. Previously, we found that XRD analysis was not sensitive enough to detect low concentrations of cobalt carbide [30].

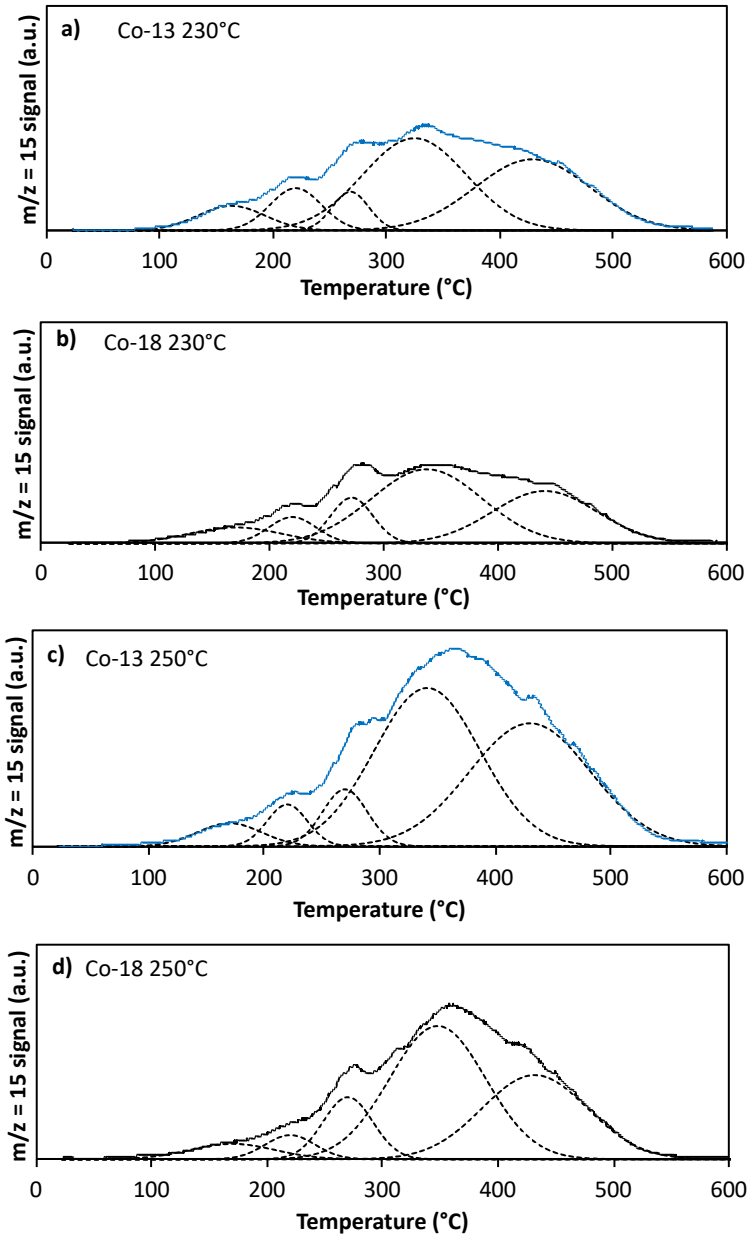

Figure 3: TPH profiles of the 230°C (a,b) and 250°C (c,d) ethylene treated catalysts.

TPH profiles can be used to quantify the amount of carbon deposited on each sample [25]. The deleterious carbon [7] (heavy hydrocarbons and polymeric carbon) amount has thus been estimated on each sample, and the obtained values are reported in Table 2. The quantities are quite comparable to those measured by Moodley et al. [7] on a 6-month aged cobalt catalyst under industrial conditions (2 wt.%). Besides, in addition to the increase of the amount of carbon deposit with temperature, higher quantities of polymeric carbon are measured on Co-13 catalyst than on Co-18 one. This is in line with Raman spectroscopy results, from which we concluded that the carbon deposited on Co-13 catalysts was more graphitic, *i.e.* with less

defaults. To give a better idea of what the obtained quantities represent, they were converted into a number of carbon surface monolayers ML_c (Table 2) by calculating the moles of carbon per mole of metallic surface cobalt atoms:

$$ML_C = \frac{N_C \cdot M_{Co}}{0.15 \cdot DOR \cdot D_{Co}} \qquad \text{(Eq. 1)}$$

where N_C represents the amount of deposited carbon ($mol \cdot g^{-1}$), M_{Co} the cobalt molar weight ($g \cdot mol^{-1}$), DOR the catalysts degree of reduction (60% [34]), 0.15 corresponds to the Co fraction on the catalyst (15 wt.%) and D_{Co} the cobalt dispersion, calculated as $1.0/d_{Co}$, with d_{Co} the metallic cobalt particle size (nm).

The calculations show that the amount of deposited carbon represents several monolayers (7 to 12), indicating that if carbon is formed on cobalt particles it necessarily migrates toward the support or forms carbon aggregates, as illustrated in Figure 4.

Table 2: Amount of deleterious carbon deposited on ethylene treated catalysts (in mass fraction and number of monolayers on the cobalt phase (ML)).

	Co-18		Co-13	
	wt.%	ML_C	wt.%	ML_C
230°C treated	0.8	7	1.1	7
250°C treated	1.3	12	2.0	12

The carbon migration toward the support has been already reported by Moodley et al. [7], who observed by TEM the presence of polymeric carbon on the alumina support of a used catalyst. It can also be noted that for a given ethylene treatment temperature, the number of monolayers is equivalent for both catalysts (*i.e.* the amount of carbon per metallic cobalt surface area is similar). This could signify that the quantity of deleterious carbon deposited is proportional to the number of initial active sites of the catalyst.

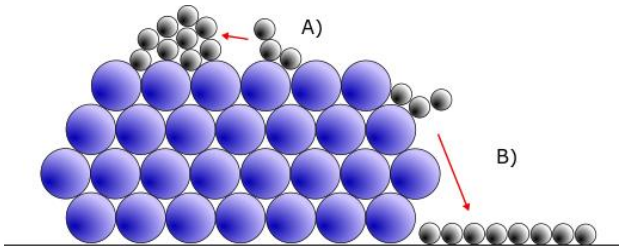

Figure 4: Hypothetical carbon migration mechanisms: A) aggregates formation, B) migration toward the catalyst's support

3.2.3 N_2 physisorption

Carbon deposition is sometimes associated with catalysts pore plugging that causes deactivation [9,26,40,41]. This phenomenon can be verified by N_2 physisorption. Table 3 compares the Co-18 catalyst texture before and after exposure to ethylene. No significant change of the specific surface area or the pore volume is detected. The carbon deposited by exposure to ethylene is thus not generated in a sufficient amount to completely obstruct the pores. The N_2 probe molecule is, however, smaller than long chain hydrocarbons, therefore partial obstruction for the diffusion of these larger molecules during FTS cannot be completely ruled out.

Table 3: Ethylene treatment effect on catalysts textural properties and number of cobalt surface sites.

		S_{BET} (m^2/g)	V_p (ml/g)	N_S ($mmol \cdot g^{-1}$)
Co-18	after reduction	141 ± 7	0.39 ± 0.01	0.05 ± 0.01
	after 230°C ethylene treatment	141 ± 7	0.37 ± 0.01	0.02 ± 0.01
	after 250°C ethylene treatment	141 ± 7	0.37 ± 0.01	0.02 ± 0.01
Co-13	after reduction	-	-	0.10 ± 0.01
	after 230°C ethylene treatment	-	-	0.03 ± 0.01
	after 250°C ethylene treatment	-	-	0.00 ± 0.01

3.2.4 CO chemisorption

Although the carbon deposit does not induce any major pore plugging, the site accessibility could still be affected by the presence of carbon species at the cobalt surface [38]. Dynamic CO chemisorption has thus been performed to quantify the number of cobalt surface sites. The number of cobalt surface sites N_s measured on reduced and treated catalysts are reported in Table 3. Firstly, it can be observed that the Co-13 catalyst has twice more cobalt surface sites than the Co-18 one, which is consistent with its higher dispersion. Secondly, the results clearly show that the carbon deposit decreases the number of sites able to adsorb CO. The Co-18 catalyst loses 60% of these sites, whatever the ethylene treatment temperature (230 or 250°C), and the Co-13 one 70% and 100% after the 230°C and 250°C ethylene treatments, respectively. It is, however, difficult to draw a correlation between the amount of deposited

carbon and the loss of cobalt surface sites, the accuracy of this method is relatively low (0.01 $mmol \cdot g^{-1}$). Besides, since this analysis has been carried out right after the ethylene treatment (without syngas re-exposure), both reversibly and irreversibly blocked sites are quantified. The loss of cobalt surface sites is therefore overestimated.

3.2.5 Diffuse Reflectance Infrared Fourier Transformed Spectroscopy (DRIFTS)

Additionally to physical blocking of some of the active sites, the adsorbed species could affect the electronic properties [28,42] of the cobalt particles. Infrared spectra of adsorbed CO on cobalt can reveal changes in the electronic structure of the cobalt particles [43]. The spectra of adsorbed CO on the Co-18 catalyst were registered before, during and after the exposure to ethylene at 230°C using the DRIFT cell.

Figure 5a shows the evolution of the spectra observed at the beginning and during ethylene treatment and Figure 5b during syngas re-exposure. Initially (*i.e.* after 24 h of syngas exposure), both bridged and linear CO adsorption modes are detected [44–47], in the respective ranges 1700 – 2000 cm^{-1} and 2000 – 2100 cm^{-1}. Before introducing ethylene, the syngas was replaced by He for 10 minutes and a relatively limited signal decrease is observed. When pure ethylene is introduced, its roto-vibrational spectrum is clearly observed [48] at 1900 cm^{-1}, and a fast decrease of the signal corresponding to adsorbed CO is detected. After 2 minutes of exposure to ethylene, no more adsorbed CO is present. During the next 3 h of ethylene exposure, no further change in signal is detected.

When ethylene is replaced by syngas (Figure 5b), no adsorbed CO signal is initially detected, indicating a completely blocked cobalt surface unable to adsorb CO [43,49]. However, during the next hours of syngas re-exposure, an increase of the adsorbed CO signal is gradually observed. This shows that some cobalt surface sites are reversibly blocked, probably because of the presence of H_2 that hydrogenates carbon compounds at a low hydrogenation temperature (< 250°C). Yet, this evolution slows down after several hours of syngas exposure and the initial signal intensity is not fully recovered. This indicates that some of the cobalt surface sites are lost irreversibly after the ethylene treatment. Interestingly, the maximum position of the adsorbed CO signal is shifted toward lower wavenumbers after exposure to ethylene. Several phenomena can be at the origin of this behaviour: the increase of the CO adsorption strength [50], reduction of cobalt oxide particles [51, 52], or a decrease of the coupling between adsorbed CO molecules [53]. The increase of adsorption strength seems unlikely, several studies [10,28,42] have reported a decrease of the Co-CO bond strength when carbon was present at the cobalt surface. The observed signal shift is therefore not attributed to

an electronic effect of the carbon deposit on CO adsorption. The reduction of small oxide particles by ethylene could, however, explain this shift, leading to highly defective cobalt particles. Zhai et al. [24] have indeed observed by XRD an increase of the metallic cobalt fraction after ethylene treatment of cobalt catalysts. The lowering of the coupling effect is also a possible explanation, since the carbon deposit decreases inevitably the number of neighbours of adsorbed CO molecules.

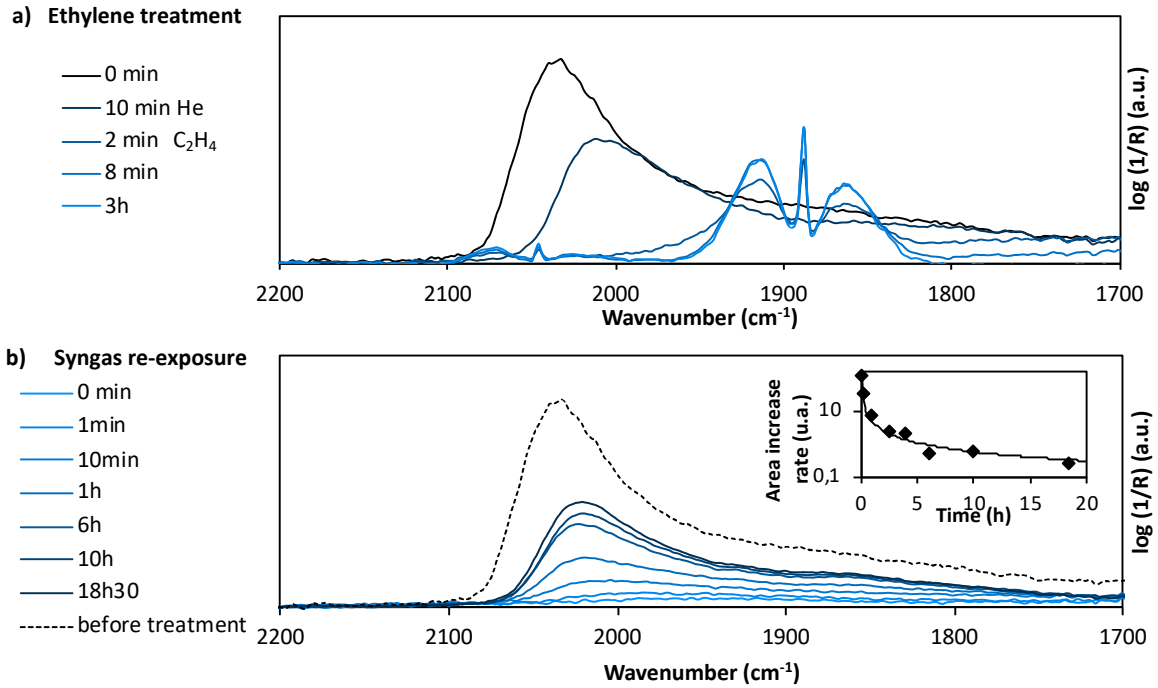

Figure 5: DRIFT spectra evolution during a) 230°C ethylene treatment and b) subsequent syngas exposure of the Co-18 catalyst, preliminarily reduced and syngas exposed for 24 h (220°C, P_{atm}, H_2/CO = 2.12).

To further compare the sites loss attributed to either linear or bridged CO adsorption modes, the signal obtained before the treatment and after 18h30 of syngas re-exposure was deconvoluted using the method described in a previous paper [30]. The linear CO adsorption capacity is found to be decreased by 53%, while that of bridged CO by 43%. These close values indicate that carbon is not preferentially deposited on a specific type of cobalt site. This observation is in qualitative agreement with DFT simulations showing that sites located either on edges or terraces can be covered by carbon species [54]

These values of loss of cobalt surface sites are slightly lower than those obtained by CO chemisorption (§ 3.2.4), since only irreversibly blocked sites were quantified by this technique.

3.3 Impact of carbon deposition on catalysts performances

It was shown above that carbon deposition induces a loss of cobalt surface sites (§ 3.2.4 and 3.2.5), thus catalyst deactivation could be expected after the ethylene treatment. The impact of carbon deposition on catalysts performances has been evaluated at 220°C, 20 barg and for a syngas composition H_2/CO = 2.12. Different syngas GHSV were operated during the test to measure both activity and selectivity at different conversion levels. Two successive tests were performed, a first one over a fresh catalyst and a second one over ethylene-treated catalyst (at 230°C and 250°C).

3.3.1 Activity

The CO consumption rates measured under the different syngas GHSV values are reported in Figure 6, for both fresh and ethylene-exposed catalysts. Replicate experiments were performed at regular intervals to verify that the fresh and ethylene-exposed catalysts remained stable. It can be observed that the conversion level does not affect significantly the CO consumption rate. The Co-13 catalyst is initially 1.5 more active than the Co-18 catalyst. This is consistent with the difference in cobalt surface area. After the ethylene treatments (*i.e.* carbon deposition), the activity of both catalysts is divided by a factor 2. This is in line with the DRIFTS results, which indicated a similar loss of cobalt surface sites of ~50%. Such deactivation levels were also observed by Zhai et al. [24] and Westrate et al. [10] on ethylene-treated cobalt catalysts. The treatment temperature has only a minor effect on the activity decrease. This is yet quite surprising, since a higher amount of polymeric carbon is deposited at higher temperature. This could be explained by carbon migration towards the support or islands formation previously mentioned, having no influence on catalytic activity.

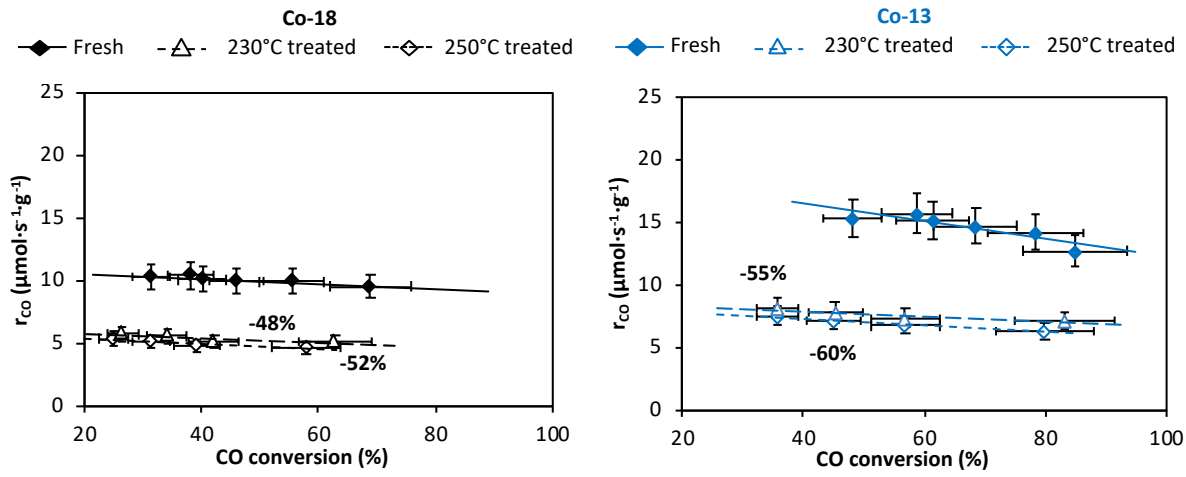

Figure 6: Co-18 (left) and Co-13 (right) catalyst activity as a function of the CO conversion, at 20 barg, 220°C, H_2/CO = 2.12. Solid and dashed lines are a guide to the eyes.

3.3.2 Selectivity

The effect of the ethylene treatment on the catalyst selectivity toward various products is presented in Figure 7. Before the ethylene treatments, the two catalysts exhibited a similar selectivity in agreement with the study of Bezemer et al. [55], who reported a cobalt particle size effect only below 8 nm. Furthermore, the effect [56–59] of the CO conversion level on the selectivity can be observed: increase of heavy compounds and CO_2 selectivity is measured when the CO conversion increases, while CH_4 and olefins selectivity decreases. This behavior is generally assumed to be due to the increase of the partial pressure of water [31,59–61], directly linked to the CO conversion level (water being a co-product of the Fischer-Tropsch synthesis).

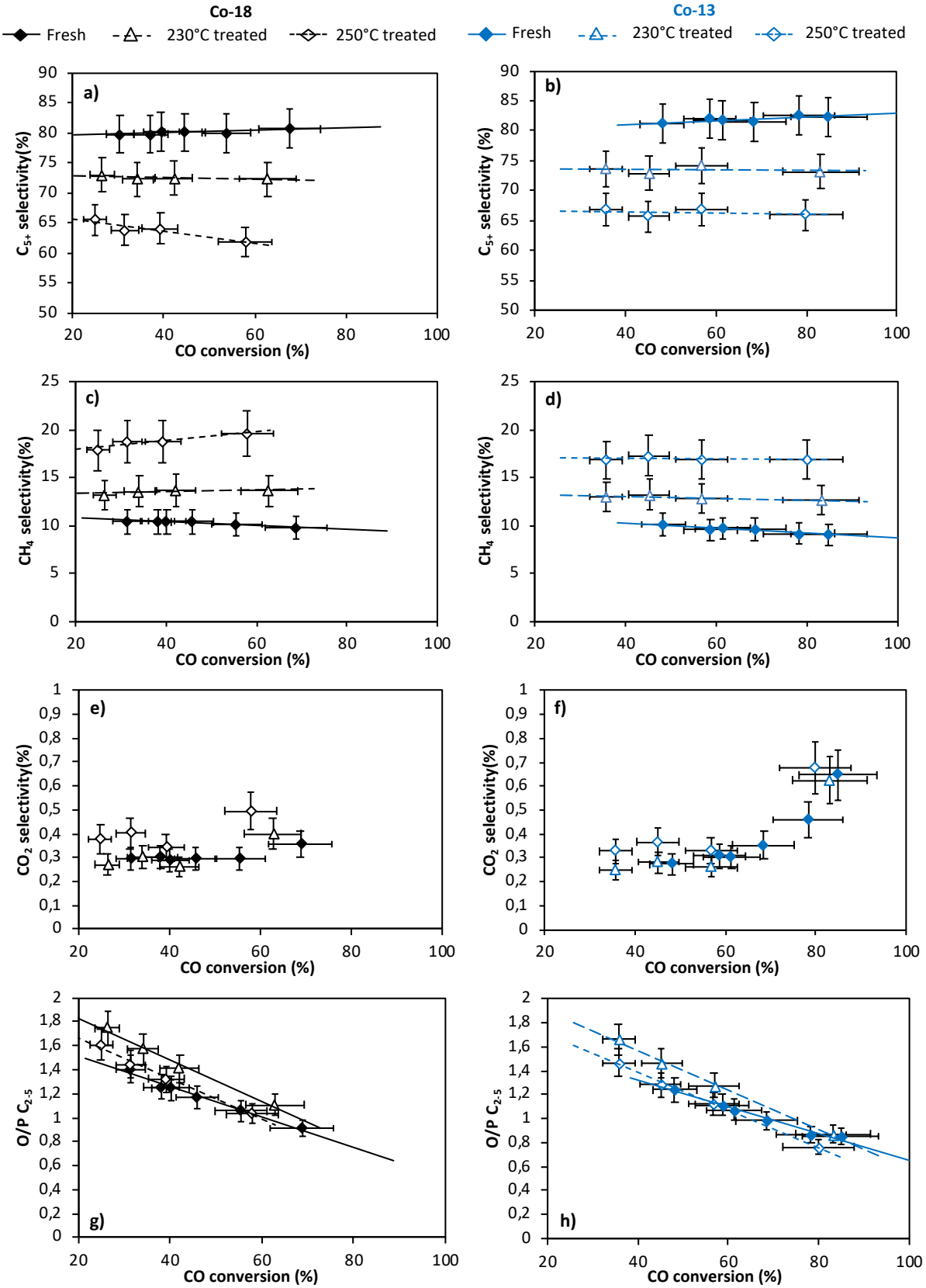

Figure 7: Co-18 (left) and Co-13 (right) catalyst selectivity of CH_4(a,b), C_{5+}(c,d), CO_2(e,f) and olefin/paraffin ratio of C_2-C_5(g,h) as a function of the CO conversion, at 20 barg, 220°C, H_2/CO = 2.12. Solid and dashed lines are a guide to the eyes.

After the ethylene treatment, a significant decrease in the C_{5+} selectivity is observed, accompanied by an increase of the CH_4 selectivity. The olefin to paraffin ratio also increases with coke deposition, but the CO_2 selectivity is not much affected by the ethylene treatment. Carbon deposition has thus a deleterious effect on the catalyst selectivity, as inferred by the studies of Sage et al. [22] and Zhai et al. [24], but in contradiction with Chen et al. [25] They [25] however, used a quite different protocol for carbon deposition, using CO instead of ethylene or acetylene. The carbon species formed may thus differ from those deposited in the present study.

Besides, the deleterious effect of carbon on the long chain hydrocarbons selectivity is also supported by *ex-situ* analysis of the liquid product fraction (Figure 8) produced over the Co-18 catalyst: the chain growth probability, α, is markedly decreased after the ethylene treatment.

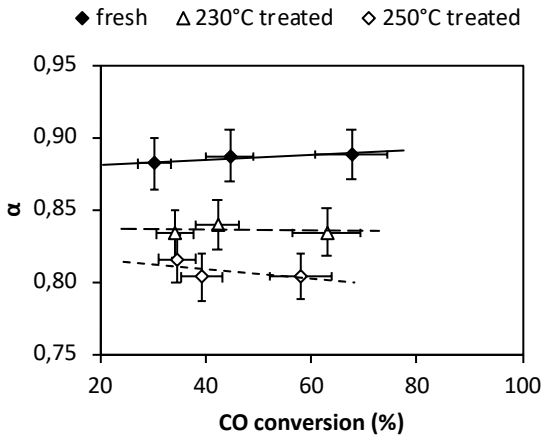

Figure 8: Co-18 chain growth probability, α, as function of the CO conversion, at 20 barg, 220°C, H_2/CO = 2.12. Solid and dashed lines are a guide to the eyes.

It is also interesting to note that, unlike deactivation, the decrease in the selectivity depends on the temperature of the ethylene treatment: the amount of polymeric carbon deposited has an effect on the deselectivation level, as illustrated on Figure 9. The reasons of this behaviour will be discussed in the next paragraph. Finally, no particular influence of the cobalt particle size is observed, with quite comparable levels of deselectivation between the two catalysts for a similar number of carbon monolayers deposited.

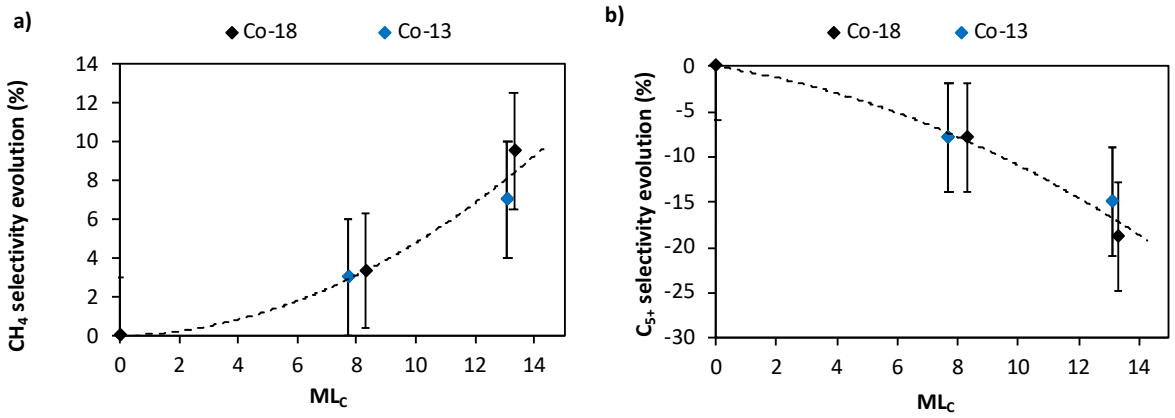

Figure 9: CH_4 (a) and C_{5+} (b) selectivity variations as a function of the number of polymeric carbon monolayers (estimated by TPH), at 220°C, 20 barg, H_2/CO = 2.12 and 50% CO conversion

4. Discussion

The loss in FT activity after the ethylene treatment is roughly proportional to the number of accessible cobalt surface atoms, determined either by CO chemisorption or DRIFTS. However, the activity does not decrease linearly with the number of calculated carbon monolayers. After the ethylene treatment at 230°C, a loss of approximately 50% of the activity is observed and this percentage hardly increases after the treatment at 250°C (see Figure 6). On the other hand, the number of carbon monolayers further increases from ~8 to ~14 theoretical monolayers with the increase of the ethylene treatment temperature. This suggests that the additional coke is either deposited on previous layers of carbon or on the support as schematized in Figure 4, but formation of subsurface carbon cannot be excluded either [5]. Raman spectroscopy showed that the nature of the carbon changes with the treatment temperature with less defects at higher treatment temperatures, indicating a more graphitic carbon. Whereas the loss in activity levels off after 8 carbon monolayers, the selectivity continues to decrease (Figure 9). While carbon-induced deactivation is certainly explained by the cobalt surface site blocking [11], the mechanisms ruling deselectivation are not straightforward. Several hypotheses can be proposed:

- Preferential deposition on certain cobalt surface sites
- Carbon induced electronic changes of the surface sites
- Steric effects

The first hypothesis is based on a two-site model for the Fischer-Tropsch synthesis, as proposed by Schulz [62]. In this model, terrace cobalt surface sites catalyze methane production, while low coordination sites favor chain growth. Such a model has been used by Chen et al. [25] to rationalize the selectivity changes that they observed after carbon deposition by CO treatments. However, these data were not collected at iso-conversion and at low CO conversion. At these conversion levels the FT selectivity strongly depends on the CO conversion [59–61,63] and the observed change in selectivity might well be due to the change in conversion rather than to the carbon deposit. Sage et al. [22] pre-treated a FT catalyst with acetylene before running FT synthesis. They observed similar changes in the selectivity as in the current study (increase of methane selectivity, decrease of the C_{5+} fraction, no effect on CO_2 and an increase of the olefins to paraffins ratio). They argued that "acetylene adsorbs preferentially on specific active sites of high coordination, which generally promote olefin re-adsorption and secondary reaction (chain growth and hydrogenation)."

The DRIFTS experiment in our case shows, however, that both linear and bridged CO adsorption sites were affected to a similar extent. Therefore, it is unlikely in the present case that different sites deactivate at different rates. This indicates that deselectivation might originate from other mechanisms. The ethylene treatment led to a similar loss of CO chemisorption sites for both cobalt particle sizes, within the experimental error. A similar loss of activity (50 vs 58%) was also found for both cobalt particles sizes. Thus, no significant particle size effect on the catalyst deactivation by carbon deposition is noticed.

Theoretical and experimental studies suggest that subsurface carbon electronically influences the CO adsorption and dissociation [5]. The change of the electronic environment, caused by the presence of carbon atoms at the surface, could modify the adsorption strength of reactants and intermediates [42,45]. This could have an effect on overall kinetics, and thus on the selectivity. Interestingly, DRIFTS experiments showed a red shift of the CO infrared band, but this was attributed to a coupling effect of carbonyl species. The deposition of carbon adatoms or the formation of superficial carbide should have instead produced a blue-shift of the carbonyl signal [44,64]. Through electronic changes the adsorption of other reactants can be altered. For instance, if the hydrogen adsorption strength is modified, the H_2/CO ratio on the catalyst surface would be affected, resulting in a modification of selectivity. A lower hydrogen coverage is consistent with the observed increase of the olefin to paraffin ratio.

The last hypothesis is the steric effect of carbon deposits, which can hinder the diffusion of monomer species and olefins and can thus slow down the formation rate of long chain hydrocarbons and decrease the chain growth probability [65]. Carbon deposits would also affect

the hydrogen coverage. Hydrogen is adsorbed dissociatively on cobalt and requires adjacent sites. If the number of surface sites decreases, the number of adjacent sites will decrease more than proportionally and the hydrogen coverage will be lower. As for the electronic effect, this will lower the olefin to paraffin ratio. DFT calculations showed that surface reconstruction can occur through the formation of a carbide-like phase, leading to a loss in selectivity [54]. It is unclear, however, why the selectivity continues to change with increasing carbon deposit, while the number of CO adsorption sites and the activity level off.

5. Conclusions

Polymeric carbon was deposited by ethylene treatments on supported cobalt catalysts with different cobalt particle sizes. TPH and Raman spectroscopy analyses of the carbon were found to be similar as the deactivating species formed during Fischer-Tropsch synthesis. The amount of polymeric carbon formed depended on the ethylene treatment temperature, but also on the cobalt particle size. While no pore plugging was detected on either catalyst, a significant loss of CO adsorption sites was measured. High-throughput experimentation was employed to compare the performance of the non-treated and ethylene treated cobalt catalysts for FTS. Data were collected at different contact times to compare selectivities at iso-conversion levels. Ethylene treated catalysts showed much lower activity. The loss in activity was roughly proportional to the loss of CO adsorption sites. Additionally, a decrease of the heavy products selectivity, an increase in the methane selectivity and a decrease of the olefin to paraffin ratio was observed after the ethylene treatments. Unlike the loss in activity, the deselectivation level was found to depend on the amount of deposited carbon. This phenomenon can be explained by a steric effect of the deposit on the diffusion of intermediates and/or products, but an electronic effect cannot be excluded, but remains difficult to prove.

References

[1] M. Argyle, C. Bartholomew, Heterogeneous Catalyst Deactivation and Regeneration, Catalysts 5 (2015) 145–269.

[2] C. Boyer, J. Gazarian, V. Lecocq, S. Maury, A. Forret, J.M. Schweitzer, V. Souchon, Development of the Fischer-Tropsch Process: From the Reaction Concept to the Process Book, Oil Gas Sci. Technol. – Rev. IFP Energies nouvelles 71 (2016) 44.

[3] van der Laan, Gerard P., Beenackers, A. A. C. M., Kinetics and Selectivity of the Fischer–Tropsch Synthesis, Catalysis Reviews 41 (1999) 255–318.

[4] N.E. Tsakoumis, M. Rønning, Ø. Borg, E. Rytter, A. Holmen, Deactivation of cobalt based Fischer–Tropsch catalysts, Catalysis Today 154 (2010) 162–182.
[5] A.M. Saib, D.J. Moodley, I.M. Ciobîcă, M.M. Hauman, B.H. Sigwebela, C.J. Weststrate, J.W. Niemantsverdriet, J. van de Loosdrecht, Fundamental understanding of deactivation and regeneration of cobalt Fischer–Tropsch synthesis catalysts, Catalysis Today 154 (2010) 271–282.
[6] E. Rytter, A. Holmen, Deactivation and Regeneration of Commercial Type Fischer-Tropsch Co-Catalysts—A Mini-Review, Catalysts 5 (2015) 478–499.
[7] D.J. Moodley, J. van de Loosdrecht, A.M. Saib, M.J. Overett, A.K. Datye, J.W. Niemantsverdriet, Carbon deposition as a deactivation mechanism of cobalt-based Fischer–Tropsch synthesis catalysts under realistic conditions, Applied Catalysis A: General 354 (2009) 102–110.
[8] C.-I. Ahn, H.M. Koo, M. Jin, J.M. Kim, T. Kim, Y.-W. Suh, K.J. Yoon, J.W. Bae, Catalyst deactivation by carbon formation during CO hydrogenation to hydrocarbons on mesoporous Co3O4, Microporous and Mesoporous Materials 188 (2014) 196–202.
[9] K. Keyvanloo, M.J. Fisher, W.C. Hecker, R.J. Lancee, G. Jacobs, C.H. Bartholomew, Kinetics of deactivation by carbon of a cobalt Fischer–Tropsch catalyst, Journal of Catalysis 327 (2015) 33–47.
[10] C.J. Weststrate, I.M. Ciobîcă, A.M. Saib, D.J. Moodley, J.W. Niemantsverdriet, Fundamental issues on practical Fischer–Tropsch catalysts, Catalysis Today 228 (2014) 106–112.
[11] S. Kocić, M. Corral Valero, J.-M. Schweitzer, P. Raybaud, Surface speciation of Co based Fischer-Tropsch catalyst under reaction conditions: Deactivation by coke or by oxidation?, Applied Catalysis A: General 590 (2020) 117332.
[12] O. Ducreux, J. Lynch, B. Rebours, M. Roy, P. Chaumette, In Situ Characterisation of Cobalt Based Fischer-Tropsch Catalysts, in: A. Parmaliana (Ed.), Natural gas conversion V: Proceedings of the Fifth International Natural Gas Conversion Symposium, Giardini Naxos-Taormina, Italy, September 20-25, 1998, Elsevier, Amsterdam, New York, 1998, pp. 125–130.
[13] Y. Dai, F. Yu, Z. Li, Y. An, T. Lin, Y. Yang, L. Zhong, H. Wang, Y. Sun, Effect of Sodium on the Structure-Performance Relationship of Co/SiO 2 for Fischer-Tropsch Synthesis, Chin. J. Chem. 35 (2017) 918–926.
[14] M. Claeys, M.E. Dry, E. van Steen, E. Du Plessis, P.J. van Berge, A.M. Saib, D.J. Moodley, In situ magnetometer study on the formation and stability of cobalt carbide in Fischer–Tropsch synthesis, Journal of Catalysis 318 (2014) 193–202.
[15] C. Lancelot, V.V. Ordomsky, O. Stéphan, M. Sadeqzadeh, H. Karaca, M. Lacroix, D. Curulla-Ferré, F. Luck, P. Fongarland, A. Griboval-Constant, A.Y. Khodakov, Direct Evidence of Surface Oxidation of Cobalt Nanoparticles in Alumina-Supported Catalysts for Fischer–Tropsch Synthesis, ACS Catal 4 (2014) 4510–4515.
[16] J. Clarkson, P.R. Ellis, R. Humble, G.J. Kelly, M. McKenna, J. West, Deactivation of alumina supported cobalt FT catalysts during testing in a Continuous-stirred tank reactor (CSTR), Applied Catalysis A: General 550 (2018) 28–37.
[17] G.W. Huber, C.G. Guymon, T.L. Conrad, B.C. Stephenson, C.H. Bartholomew, Hydrothermal Stability of Co/SiO2 Fischer-Tropsch Synthesis Catalysts, in: J.J. Spivey, G.W. Roberts, B.H. Davis (Eds.), Catalyst Deactivation 2001, Elsevier, 2001, pp. 423–430.
[18] A.-M. Hilmen, O.A. Lindvåg, E. Bergene, D. Schanke, S. Eri, A. Holmen, Selectivity and activity changes upon water addition during Fischer-Tropsch synthesis, in: E. Iglesia, J. Spivey, T. Fleisch (Eds.), Studies in Surface Science and Catalysis Natural Gas Conversion VI, Elsevier, 2001, pp. 295–300.
[19] C.H. Bartholomew, R.M. Bowman, Sulfur poisoning of cobalt and iron fischer-tropsch catalysts, Applied Catalysis 15 (1985) 59–67.
[20] Stephen C. Leviness, Charles J. Mart, William C. Behrmann, Stephen J. Hsia, Daniel R. Neskora, Slurry hydrocarbon synthesis process with increased catalyst life, US6284807B1 (2001), ExxonMobil Research and Engineering Co.
[21] G.A. Somorjai, M.A. van Hove, Adsorbate-induced restructuring of surfaces, Progress in Surface Science 30 (1989) 201–231.
[22] V. Sage, Y. Sun, P. Hazewinkel, T. Bhatelia, L. Braconnier, L. Tang, K. Chiang, M. Batten, N. Burke, Modified product selectivity in Fischer-Tropsch synthesis by catalyst pre-treatment, Fuel Processing Technology 167 (2017) 183–192.
[23] K. Fei Tan, J. Xu, J. Chang, A. Borgna, M. Saeys, Carbon deposition on Co catalysts during Fischer–Tropsch synthesis, Journal of Catalysis 274 (2010) 121–129.
[24] P. Zhai, P.-P. Chen, J. Xie, J.-X. Liu, H. Zhao, L. Lin, B. Zhao, H.-Y. Su, Q. Zhu, W.-X. Li, D. Ma, Carbon induced selective regulation of cobalt-based Fischer-Tropsch catalysts by ethylene treatment, Faraday discussions 197 (2017) 207–224.
[25] W. Chen, T.F. Kimpel, Y. Song, F.-K. Chiang, B. Zijlstra, R. Pestman, P. Wang, E.J.M. Hensen, Influence of Carbon Deposits on the Cobalt-Catalyzed Fischer-Tropsch Reaction: Evidence of a Two-Site Reaction Model, ACS catalysis 8 (2018) 1580–1590.
[26] C.H. Bartholomew, Mechanisms of catalyst deactivation, Applied Catalysis A: General 212 (2001) 17–60.
[27] L. Xu, Y. Ma, Z. Wu, B. Chen, Q. Yuan, W. Huang, A Photoemission Study of Ethylene Decomposition on a Co(0001) Surface, J. Phys. Chem. C 116 (2012) 4167–4174.

[28] L. Xu, Y. Ma, Y. Zhang, B. Chen, Z. Wu, Z. Jiang, W. Huang, Surface Chemistry of C 2 H 4 CO, and H 2 on Clean and Graphite Carbon-Modified Co(0001) Surfaces, J. Phys. Chem. C 115 (2011) 3416–3424.
[29] C.J. Weststrate, A.C. Kızılkaya, E.T.R. Rossen, Verhoeven, Martinus W. G. M., I.M. Ciobîcă, A.M. Saib, J.W. Niemantsverdriet, Atomic and Polymeric Carbon on Co(0001), J. Phys. Chem. C 116 (2012) 11575–11583.
[30] P. Hazemann, D. Decottignies, S. Maury, S. Humbert, F.C. Meunier, Y. Schuurman, Selectivity loss in Fischer-Tropsch synthesis: The effect of cobalt carbide formation, Journal of Catalysis 397 (2021) 1–12.
[31] Branislav Todic, Wenping Ma, Gary Jacobs, Burtron H. Davis, Dragomir B. Bukur, Effect of process conditions on the product distribution of Fischer–Tropsch synthesis over a Re-promoted cobalt-alumina catalyst using a stirred tank slurry reactor, Journal of Catalysis 311 (2014) 325–338.
[32] A. Paredes-Nunez, I. Jbir, D. Bianchi, F.C. Meunier, Spectrum baseline artefacts and correction of gas-phase species signal during diffuse reflectance FT-IR analyses of catalysts at variable temperatures, Applied Catalysis A: General 495 (2015) 17–22.
[33] J. Sirita, S. Phanichphant, F.C. Meunier, Quantitative analysis of adsorbate concentrations by diffuse reflectance FT-IR, Analytical chemistry 79 (2007) 3912–3918.
[34] P. Hazemann, D. Decottignies, S. Maury, S. Humbert, A. Berliet, C. Daniel, Y. Schuurman, Kinetic data acquisition in high-throughput Fischer–Tropsch experimentation, Catal. Sci. Technol. 10 (2020) 7331–7343.
[35] R.B. Anderson, R.A. Friedel, H.H. Storch, Fischer-Tropsch Reaction Mechanism Involving Stepwise Growth of Carbon Chain, The Journal of Chemical Physics 19 (1951) 313–319.
[36] K.H. Cats, B.M. Weckhuysen, Combined Operando X-ray Diffraction/Raman Spectroscopy of Catalytic Solids in the Laboratory, ChemCatChem 8 (2016) 1531–1542.
[37] H. Xiong, M.A. Motchelaho, M. Moyo, L.L. Jewell, N.J. Coville, Cobalt catalysts supported on a micro-coil carbon in Fischer–Tropsch synthesis, Catalysis Today 214 (2013) 50–60.
[38] A. Carvalho, V.V. Ordomsky, Y. Luo, M. Marinova, A.R. Muniz, N.R. Marcilio, A.Y. Khodakov, Elucidation of deactivation phenomena in cobalt catalyst for Fischer-Tropsch synthesis using SSITKA, Journal of Catalysis 344 (2016) 669–679.
[39] L. Pinard, P. Bichon, A. Popov, J.L. Lemberton, C. Canaff, F. Maugé, P. Bazin, E.F. S.-Aguiar, P. Magnoux, Identification of the carbonaceous compounds present on a deactivated cobalt based Fischer–Trospch catalyst resistant to “rejuvenation treatment”, Applied Catalysis A: General 406 (2011) 73–80.
[40] D. Peña, A. Griboval-Constant, C. Lancelot, M. Quijada, N. Visez, O. Stéphan, V. Lecocq, F. Diehl, A.Y. Khodakov, Molecular structure and localization of carbon species in alumina supported cobalt Fischer–Tropsch catalysts in a slurry reactor, Catalysis Today 228 (2014) 65–76.
[41] D. Peña, A. Griboval-Constant, V. Lecocq, F. Diehl, A.Y. Khodakov, Influence of operating conditions in a continuously stirred tank reactor on the formation of carbon species on alumina supported cobalt Fischer–Tropsch catalysts, Catalysis Today 215 (2013) 43–51.
[42] L. Joos, I.A.W. Filot, S. Cottenier, E.J.M. Hensen, M. Waroquier, V. van Speybroeck, R.A. van Santen, Reactivity of CO on Carbon-Covered Cobalt Surfaces in Fischer–Tropsch Synthesis, J. Phys. Chem. C 118 (2014) 5317–5327.
[43] A. Paredes-Nunez, D. Lorito, Y. Schuurman, N. Guilhaume, F.C. Meunier, Origins of the poisoning effect of chlorine on the CO hydrogenation activity of alumina-supported cobalt monitored by operando FT-IR spectroscopy, Journal of Catalysis 329 (2015) 229–236.
[44] J. Couble, D. Bianchi, Experimental Microkinetic Approach of the Surface Reconstruction of Cobalt Particles in Relationship with the CO/H 2 Reaction on a Reduced 10% Co/Al 2 O 3 Catalyst, J. Phys. Chem. C 117 (2013) 14544–14557.
[45] A. Paredes-Nunez, D. Lorito, N. Guilhaume, C. Mirodatos, Y. Schuurman, F.C. Meunier, Nature and reactivity of the surface species observed over a supported cobalt catalyst under CO/H2 mixtures, Catalysis Today 242 (2015) 178–183.
[46] M.J. Dees, T. Shido, Y. Iwasawa, V. Ponec, Infrared studies of CO adsorbed on supported Pt・Co catalysts, Journal of Catalysis 124 (1990) 530–540.
[47] D. Song, J. Li, Q. Cai, In Situ Diffuse Reflectance FTIR Study of CO Adsorbed on a Cobalt Catalyst Supported by Silica with Different Pore Sizes, J. Phys. Chem. C 111 (2007) 18970–18979.
[48] Antony Williams, ChemSpider: Ethylene, http://www.chemspider.com/Chemical-Structure.6085.html?rid=db25fa1b-6fbe-4479-ba2d-4dc172c6bae5.
[49] A. Paredes-Nunez, D. Lorito, L. Burel, D. Motta-Meira, G. Agostini, N. Guilhaume, Y. Schuurman, F. Meunier, CO Hydrogenation on Cobalt-Based Catalysts, Angewandte Chemie (International ed. in English) 57 (2018) 547–550.
[50] G. Blyholder, Molecular Orbital View of Chemisorbed Carbon Monoxide, The Journal of Physical Chemistry 68 (1964) 2772–2777.
[51] Khodakov, A. Y., et al., Reducibility of Cobalt Species in Silica-Supported Fischer–Tropsch Catalysts (1997) 16–25.

[52] B. Mothebe, D.J. Duvenhage, V.D. Sokolovskii, N.J. Coville, DRIFTS studies on Co/TiO2 Fischer-Tropsch catalysts, in: M. de Pontes, R. Espinoza, C. Nicolaides, J. Scholtz, M. Scurrell (Eds.), Studies in Surface Science and Catalysis Natural Gas Conversion IV, Elsevier, 1997, pp. 187–192.
[53] V.M. Browne, S.G. Fox, P. Hollins, Coupling effects in infrared spectra from supported metal catalyts, Materials Chemistry and Physics 29 (1991) 235–244.
[54] M. Corral Valero, P. Raybaud, Stability of Carbon on Cobalt Surfaces in Fischer–Tropsch Reaction Conditions, J. Phys. Chem. C 118 (2014) 22479–22490.
[55] G.L. Bezemer, J.H. Bitter, Kuipers, Herman P. C. E., H. Oosterbeek, J.E. Holewijn, X. Xu, F. Kapteijn, A.J. van Dillen, K.P. de Jong, Cobalt Particle Size Effects in the Fischer−Tropsch Reaction Studied with Carbon Nanofiber Supported Catalysts, J. Am. Chem. Soc. 128 (2006) 3956–3964.
[56] A. Lillebø, E. Rytter, E.A. Blekkan, A. Holmen, Fischer–Tropsch Synthesis at High Conversions on Al2O3-Supported Co Catalysts with Different H2/CO Levels, Ind. Eng. Chem. Res. 56 (2017) 13281–13286.
[57] D.B. Bukur, Z. Pan, W. Ma, G. Jacobs, B.H. Davis, Effect of CO Conversion on the Product Distribution of a Co/Al2O3 Fischer–Tropsch Synthesis Catalyst Using a Fixed Bed Reactor, Catal Lett 142 (2012) 1382–1387.
[58] W. Ma, G. Jacobs, Y. Ji, T. Bhatelia, D.B. Bukur, S. Khalid, B.H. Davis, Fischer–Tropsch Synthesis, Top Catal 54 (2011) 757–767.
[59] S. Storsæter, Ø. Borg, E.A. Blekkan, A. Holmen, Study of the effect of water on Fischer–Tropsch synthesis over supported cobalt catalysts, Journal of Catalysis 231 (2005) 405–419.
[60] S. Lögdberg, M. Lualdi, S. Järås, J.C. Walmsley, E.A. Blekkan, E. Rytter, A. Holmen, On the selectivity of cobalt-based Fischer–Tropsch catalysts, Journal of Catalysis 274 (2010) 84–98.
[61] F.G. Botes, Influences of Water and Syngas Partial Pressure on the Kinetics of a Commercial Alumina-Supported Cobalt Fischer−Tropsch Catalyst, Ind. Eng. Chem. Res. 48 (2009) 1859–1865.
[62] H. Schulz, Major and Minor Reactions in Fischer–Tropsch Synthesis on Cobalt Catalysts, Topics in Catalysis 26 (2003) 73–85.
[63] E. Rebmann, P. Fongarland, V. Lecocq, F. Diehl, Y. Schuurman, Measurement of the Influence of the Microstructure of Alumina-Supported Cobalt Catalysts on their Activity and Selectivity in Fischer-Tropsch Synthesis by using Steady-State and Transient Kinetics, ChemCatChem 9 (2017) 2344–2351.
[64] B. Ernst, A. Bensaddik, L. Hilaire, P. Chaumette, A. Kiennemann, Study on a cobalt silica catalyst during reduction and Fischer–Tropsch reaction: In situ EXAFS compared to XPS and XRD, Catalysis Today 39 (1998) 329–341.
[65] E. Rytter, N.E. Tsakoumis, A. Holmen, On the selectivity to higher hydrocarbons in Co-based Fischer–Tropsch synthesis, Catalysis Today 261 (2016) 3–16.